A21N-2751: Identification of Linear and Nonlinear Causal Relationship Among Low-Frequency Climatic Phenomena in the Last Millennium.

Lucas Massarope[1] (lucasmassarope@gmail.com); Maria Gabriela Louzada Malfatti[2]; Igor Stivanelli Custódio[1]; Pedro Leite da Silva Dias[1]

[1]Institute of Astronomy, Geophysics and Atmospheric Sciences, University of São Paulo; [2]Institute of Energy and Environment, University of São Paulo.

INTRODUCTION

- In meteorology, identification of teleconnections between climatic patterns plays an important role in the validation of atmospheric models which are used for weather and climate prediction and for the development of future climate scenarios under global warming forcing.
- In order to evaluate the connectivity between climatic patterns, correlation analysis is often used, but this type of analysis may lead to oversimplified relationships, which do not imply causality between different scales of time (i.e., a nonlinearity).
- In this work, Partial Directed Coherence (PDC) and kernel non-linear Partial Directed Coherence (*kn*PDC) were used to infer the influence between atmospheric compartments (atmosphere and ocean), allowing the detection of linear and non-linear connections, respectively, between variables representative of important climatic variability modes in the PMIP3 simulations for the last millennium.

DATA AND METHODOLOGY

Climate Indices (Last Millennium: years 850 to 1850)

Weighted average set of climate model simulations of PMIP3
PMIP3: represent past climate simulations provided by the climate models of CMIP5.

Groups of climatic indicators

El Niño-Southern Oscillation (ENSO); Atlantic Multidecadal Oscillation (AMO); Atlantic Interhemispheric SST Gradient (GTA)	Antarctic Oscillation (AAO); *El Niño-Southern Oscillation* (ENSO); Pacific-South American (PSA1, EOF2); Quasi-Biennial (QBO)

Inference of the linear or nonlinear couplings between the climatological patterns

Partial Directed Coherence (PDC) [1]	Nonlinear Partial Directed Coherence kernel (*kn*PDC) [2]

We represent the input series $\{x_i(n)\}_{n=1}^{N}$ (input space) through a Kernel Vector Autoregressive (kVAR) model, such as (Massaroppe and Baccalá, 2019)

$$\langle\phi(x(n))| = \sum_{r=1}^{p} A_k\langle\phi(x(n-k))| + \langle\tilde{w}(n)|,$$

where

- $\{\langle\tilde{w}(n)|\}_{n\in\mathbb{Z}} \sim i.i.d.\,WN(0,\Sigma_{\langle\tilde{w}(n)\rangle})$
- $\phi : \mathbb{X} \rightarrow \mathbb{F}$ represents a nonlinear mapping (Parzen, 1959), such that $\mathbb{E}\{\langle\phi[x_i(n)]|\phi[x_i(n-k)]\rangle\} = \mathbb{E}\{\kappa[x_i(n), x_i(n-k)]\}$;
- $\kappa(\cdot)$: a Mercer kernel;
- $\langle\cdot|\cdot\rangle$: Dirac's ´bracket´ notation.

The *kernel-nonlinear*-Partial Directed Coherence defined, in the phase space, as

$$_{\kappa\eta}\pi_{ij}(f) = \frac{\bar{A}_{ij}(f)/\sqrt{\sigma_{ii}}}{\sqrt{\bar{a}_j^H(f)\Sigma_{\langle\tilde{w}(n)\rangle}^{-1}\bar{a}_j(f)}}$$

where

- $\bar{A}_{ij}^{\phi}(f) = \delta_{ij} - \sum_{r=1}^{p} a_{ij}^{\phi}(r)e^{-i2\pi fr}, (i^2 = -1)$;
- $a_{ij}^{\phi}(\mathrm{r})$ are the coefficients of na adequately fit *k*VAR model;
- $\bar{a}_j(f)$ represent the columns of the $\left[\bar{A}_{ij}^{\phi}(f)\right]$ matrix.

PDC is similarly defined and can be seen in (Baccalá et al.,2013).

RESULTS

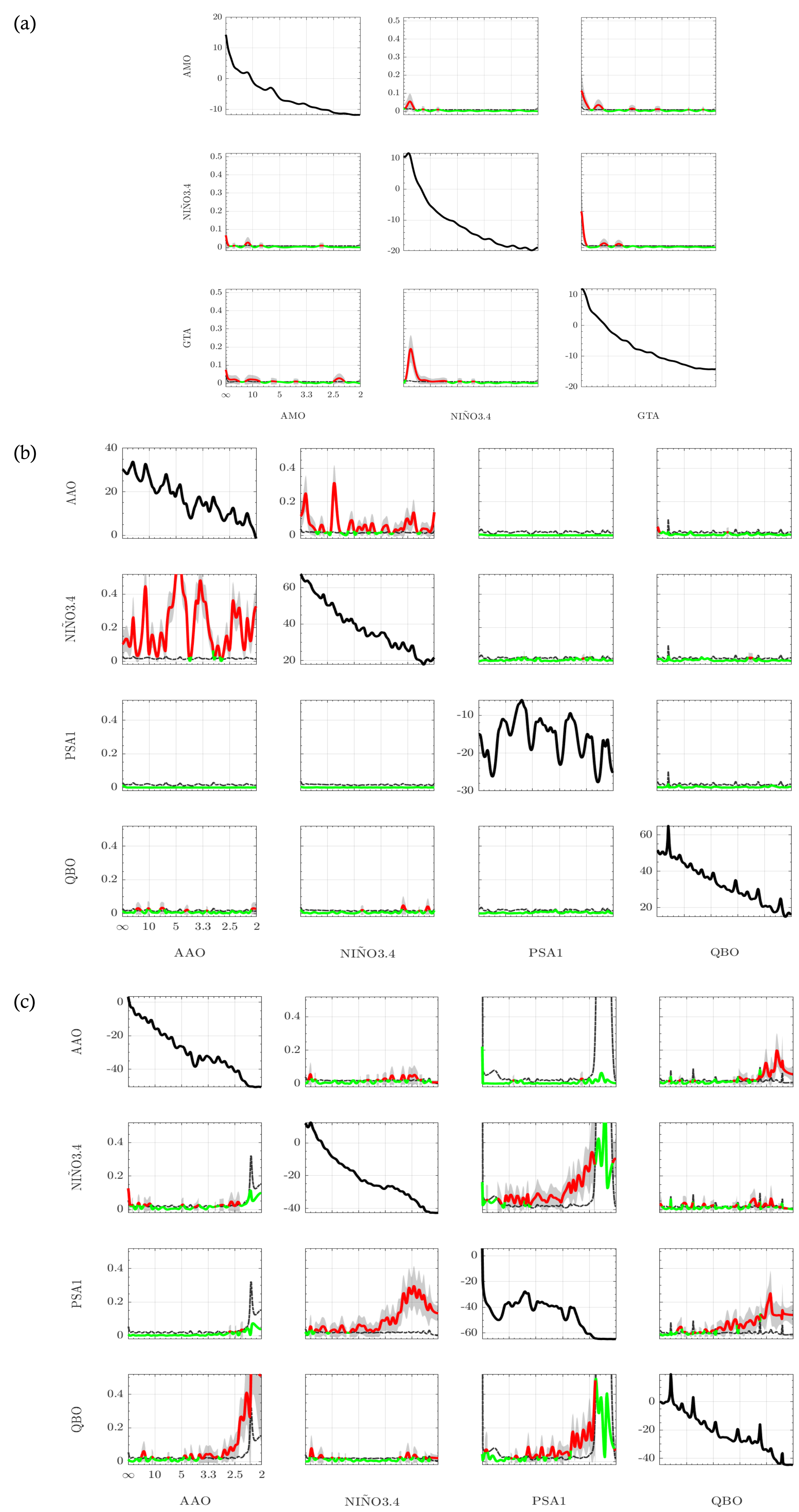

Fig. 1. The black line represents the (pseudo-) spectral density of the series, in dB.; the red line represents the statistically significant PDC / *kn*PDC values; the dashed black line represents Patnaik's threshold approximation (Baccalá et al., 2013); the green line the statistically non-significant PDC / knPDC values. Therefore, using 1% significance level, the figures depict, respectively: (a) PDC for time series set (AMO, Niño 3.4 and GTA) using an autoregressive model of order p = 48, (b) PDC for time series set (AAO, Niño 3.4, PSA1 and QBO) using an autoregressive model of order p = 24 (c) *kn*PDC for the time series set (AAO, Niño 3.4, PSA1) and using the polynomial kernel $[\boldsymbol{k}(\boldsymbol{x},\boldsymbol{y}) = (\boldsymbol{x}.\boldsymbol{y})^2]$ and using a *kernel-*autoregressive model of order p = 24.

Fig.1a shows linear causality relationship (PDC) between: AMO → GTA; AMO → Niño 3.4; Niño 3.4 → GTA; Niño 3.4 → AMO; GTA → Niño 3.4; GTA → AMO. For nonlinear causality relationship (knPDC), no results were observed in the low frequency period. The observed results suggests that the Atlantic and Pacific oceans influence each other at different times.

Fig.1b depicts a linear causality relationship (PDC) between: AAO ↔ Niño 3.4; AAO ↔ QBO; Niño 3,4 → QBO. Some studies corroborate the results obtained with AAO and QBO (Gava et al., 2017), AAO and Niño 3.4 (Yu et al., 2015; Wang et al., 2017) and Niño 3.4 and QBO (Kane, 2005; Li et al., 2016).

*kn*PDC results (Fig.1c) suggests a nonlinear causal relationship between the same patterns observed in PDC, but with higher statistically significant values at high and low frequency. In addition, nonlinear causal relationships between PSA1↔Niño3.4 and PSA1↔QBO are observed. These results find support in other studies such as in Yu et al. (2015) for a relationship between PSA and ENSO and in Kane (2005) between PSA and QBO.

DISCUSSION AND CONCLUSIONS

For the first group, no significant results were observed on the low-frequency band, observing only linear relationships between the Pacific and Atlantic Oceans. For the second group, the causal analysis point to linear relationships between ENSO ⟷ AAO, and nonlinear between ENSO ⟷ PSA in the low and high band and QBO ⟷ AAO, QBO ⟷ ENSO and QBO ⟷ PSA in the low-frequency band. In summary, the results indicate a higher nonlinear connection between low-frequency phenomena.

ACKNOWLEDGMENTS

The authors gratefully acknowledge support from the FAPESP Grant 2015/50686-1 (PACMEDY Project). L.M. to CAPES Grant 88887.161474/2017-00 (PALEOCEANO Project). M.G.L.M. to CNPq Grant 2017/05285-4 (Ph.D. Scholarship). I.S.C. to FAPESP Grant 2017/05285-4 (Ph.D. Scholarship) and CNPq Grant 471700/2013-4 (Universal Project).

REFERENCES

[1] PARZEN, E. Statistical inference on time series by Hilbert space method, I. Technical Report 23, Applied Mathematics and Statistics Laboratory, Stanford University, Stanford, January 1959.

[2] MASSAROPPE, L. and BACCALÁ, L. A. Kernel methods for nonlinear connectivity detection. **Entropy**, 2019.

[3] BACCALÁ, L. A. et al. Unified asymptotic theory for all partial directed coherence forms. **Philosophical Transactions of the Royal Society A: Mathematical, Physical and Engineering Sciences**, v. 371, n. 1997, p. 20120158, 2013.

[4] LI, T. et al. Southern Hemisphere Summer Mesopause Responses to El Niño–Southern Oscillation. **Journal of Climate**, v. 29, n. 17, p. 6319-6328, 2016.

[5] GAVA, M. L. L. M.; VASCONCELLOS, F. C.; SANSIGOLO, C. A. Study of a possible relationship between the quasi-biennial oscillation and the Antarctic oscillation. In: Simpósio Internacional de Climatologia, 7., 2017. Petrópolis-RJ. **Anais…** Rio de Janeiro: SBMET, 2017.

[6] KANE, R. P. Spectral characteristics and ENSO relationship of the Paraná river streamflow. **Mausam**, v. 56, n. 2, p. 367, 2005.

[7] YU, J.; PAEK, H; SALTZMAN, E. S.; LEE, T. The early 1990s change in ENSO-PSA-SAM relationships and its impact on Southern Hemisphere Climate. **Journal of Climate**, v. 28, n, 23, p. 9393-9408, 2015.

[8] WANG, S. -Y.; YOON, J. -H.; FUNK, C. C.; GILLIES, R. R. **Climate Extremes: Patterns and Mechanisms.** 1. ed. New Jersey: John Wiley & sons, American Geophysical Union, 2017, 386 p.